Characterization of BF_2, Ga and In Dopants in Si for halo implantation

Yusuke Matsunaga[1], Siti Rahmah Binti Aid[1], Satoru Matsumoto[2], John Borland[3], and Masayasu Tanjyo[4]

[1]Department of Electronics and Electrical Engineering, Keio University,
3-14-1, Hiyoshi, Kohoku-ku, Yokohama 223-8522, Japan
[2]Department of Electronics and Electrical Engineering, Keio University,
3-14-1, Hiyoshi, Kohoku-ku, Yokohama 223-8522, Japan
Malaysia-Japan International Institute of Technology
Universiti Teknologi Malaysia Kuala Lumpur
Jalan Semarak 54100, Kualas Lumpur, Malaysia
[3]JOB Technologies, Aiea, Hawaii, USA
[4]Nissin Ion Equipment Co., LTD,
575Kuze-Tonoshiro-cho, Minami-ku, Kyoto 601-8205, Japan
Phone: +81-45-566-51548 E-mail: matumoto@elec.keio.ac.jp

1. Introduction

Ion implantation with medium current implants has been applied for halo implantation. Indium (In) has been used for halo implantation for suppression of short channel effect [1]. Recently, the advantage of cryogenic ion implantation with medium current implanters was reported [2]. They showed that the cryogenic BF_2 implant improved the short channel rolloff characteristics.

Previously, we reported [3] the dopant diffusion, electrical activation, diode characteristics and damage recovery of BF_2, Ga and In implanted Si. Diode I-V characteristics indicated that Ga implanted Si showed the good reverse characteristics compared with other dopants. However, the diode characteristic was only obtained for the dose of $3.0x10^{13}$ cm^{-2}.

On the other hand, one of the authors [4] compared BF_2, Ga, In, C+Ga and In+BF_2 dopant species for nMOS halo formation. It was reported that C+Ga co-implant showed the best results among the above dopant species from the point of a steep retrograde profile formation. In their analysis, sheet resistance and junction leakage were measured by a relatively new method of Junction Photo Voltage (JPV).

In this work, we studied the electrical characteristics of BF_2, Ga and In implanted Si under the typical conditions of implant doses and energies for halo implants. We measured the sheet carrier concentration, sheet resistance and mobility with Hall-effect measurement. We also fabricated the diodes and evaluated the forward- and reverse-biased current-voltage characteristics. The present results were compared with those of the JPV method. With TEM analysis of annealed samples, we discussed the relationship between the electrical characteristics and crystalline structures.

2. Experimental

Dopant species of B, Ga and In have been implanted into n-type Si wafers with Nissin medium current implanter. The implant energy and dose were typically used for halo implants. The details of the implant conditions are shown in Table. 1. The implant conditions were chosen to produce the almost same projected ranges and peak concentrations of as-implanted profiles for each sample.

The amorphous layer thickness of as-implanted samples was measured with ellipsometry. The values of the thickness for BF_2 and Ga implanted samples were shown in Fig. 1. As shown in Fig. 1, thickness of amorphous layer of BF2 and Ga was around 5 nm, while it was about 40 nm for In.

Annealing was performed using a 1200 C Flash anneal followed by 900 C for 10s RTA anneal.

Table 1 Implant species and conditions

Dopant species	Energy [keV]	Dose [ions/cm^2]	Electrical activation [%]
BF2	26	$1.5x10^{13}$	86.0
BF2	26	$3.0 x10^{13}$	70.3
BF2	26	$4.5 x10^{13}$	64.7
Ga	36	$1.5x10^{13}$	47.2
Ga	36	$3.0 x10^{13}$	37.7
Ga	36	$4.5 x10^{13}$	32.4
In	60	$1.5x10^{13}$	13.3
In	60	$3.0x10^{13}$	8.0
In	60	$4.5 x10^{13}$	6.8

Sheet carrier concentration and sheet resistance were measured by Hall-effect measurement. Mesa-type diodes were fabricated and the current (I) – voltage (V) characteristics were measured by HP semiconductor parameter analyzer.

The crystallinity near the junction of samples after annealing was analyzed by transmission electron microscope (TEM).

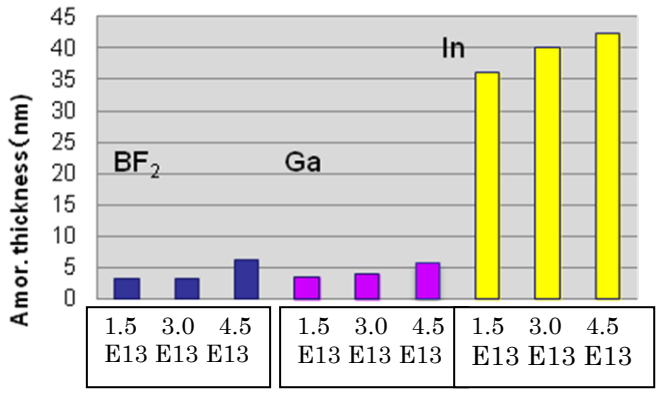

Fig. 1 Amorphous thickness of as-implanted samples

3. Results

A. Sheet Resistance

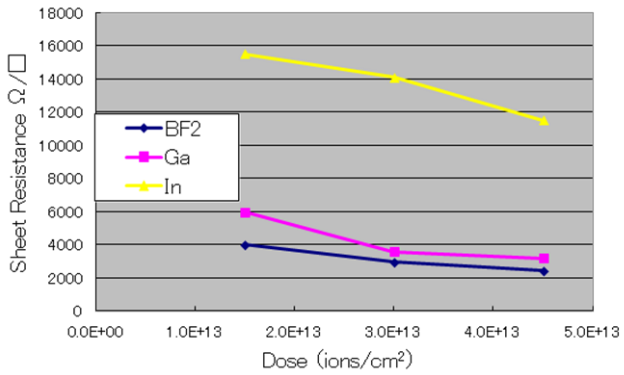

Fig. 2 Sheet Resistance vs implant dose

Figure 2 shows the sheet resistance (Rs) of BF_2, Ga and In implanted samples as a function of implant dose. Rs values of In samples are much higher than those of BF_2 and Ga by about 3-4 times. On the other hand, Rs values of BF_2 and Ga samples are almost the same. However, as shown in Table 1, electrical activation of Ga samples is almost half of that of BF_2 for respective doses. This discrepancy is considered as follows. Since sheet resistance depends on the product of carrier concentration, mobility and charge, it is necessary to include these parameters. Figure 3 shows the mobility obtained by Hall-effect measurement as a function of doses. It should be noted this mobility is an average value in the diffused region. The mobility of BF_2 is lowest among three dopants and the electrical activation is highest as shown in Table. 1. Therefore, the lower mobility value of BF_2 is due to the fact that mobility decreases with the increase of carrier concentration. Thus the sheet resistance in Fig. 2 can be interpreted with the above consideration.

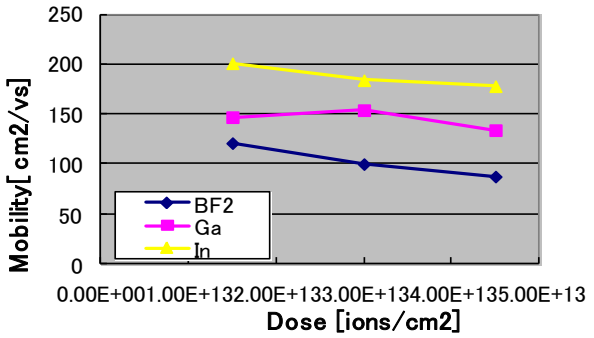

Fig. 3 Mobility as a function of dose.

B. Diode I-V characteristics

Figures 4, 5 and 6 are the diode I-V characteristics of BF_2, Ga and In for a parameter of implanted dose, respectively.

Generally, the experimental forward current, J_F, can be expressed by the following empirical form [5].

$$J_F \sim \exp(qV/nkT) \qquad (1)$$

where n is called ideality factor. The factor n equals 1 when the diffusion current dominates, while the factor n equals 2 when the recombination current dominates.

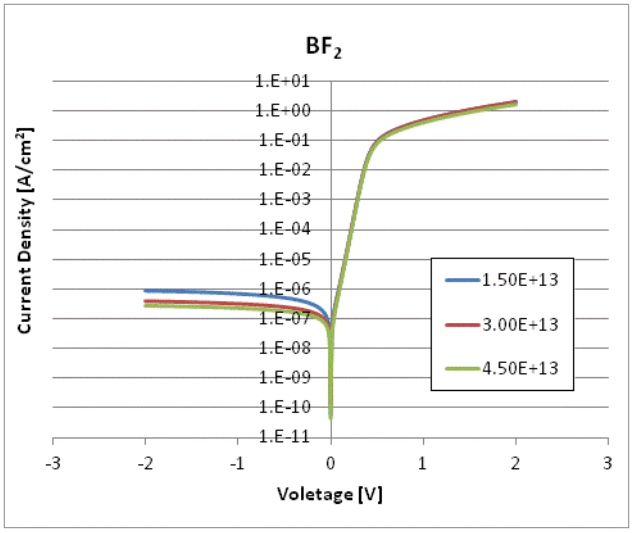

Fig. 4 I-V characteristics of BF_2.

Using Eq. (1), the factor n can be estimated from the data of forward current. The n values of BF_2 (~1.12) are very near to 1for the respective doses, while the n values of Ga and In are about 1.2 as shown in Fig. 7. When we looked forward current carefully, recombination current region is observed at the low voltage in the case of Ga and In as shown in Figs. 5 and 6.

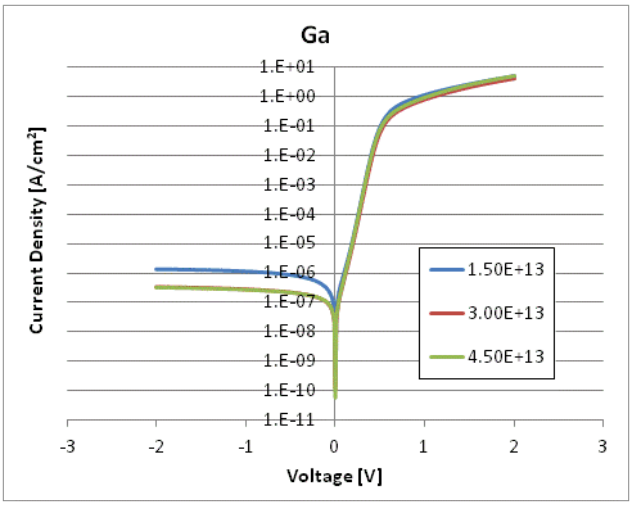

Fig. 5 I-V characteristics of Ga.

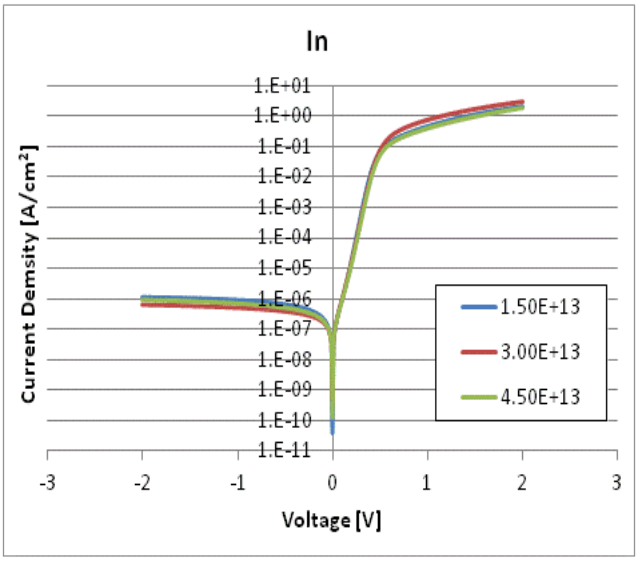

Fig. 6 I-V characteristics of In.

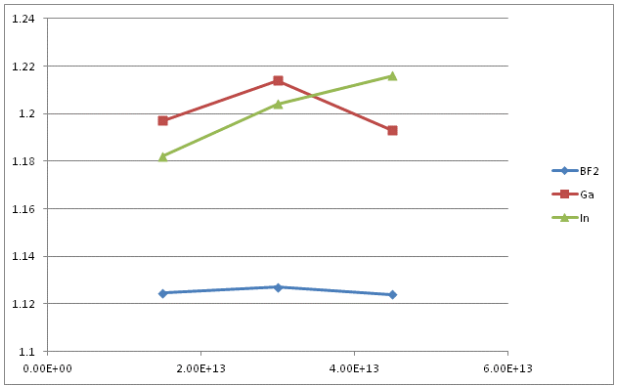

Fig. 7 The factor *n* as a function of doses.

Next, we consider the current under reverse-bias condition. In the dose of $1.5\text{x}10^{13}\text{cm}^{-2}$, the values of reverse current at -2V are to be about $1\text{x}10^{-6}$ A/cm^2, irrespective of dopant species. At the doses of $3\text{x}10^{13}$ and $4.5\text{x}10^{13}$ cm^{-2}, reverse current reduces for BF_2 and Ga samples, but In samples have still higher reverse current.

It has been reported [4] that junction leakage of In sample is lowest and BF_2 sample has the highest junction leakage from the JPV method.

As shown in Figs. 4, 5 and 6, the present results disagree with the JPV leakage trend. Regarding this point, we discuss the following section using TEM analysis.

C. Cross-sectional TEM micrograph

Figures 8, 9 and 10 are the cross-sectional TEM micrographs of BF_2, Ga and In samples after anneal. Blue dotted lines in Figs. 8 and 9 indicate the surface, and red dotted lines indicate the original amorphous layer.

As shown in Figs. 8 (BF_2) and 9 (Ga), very clear lattice images are observed from the surface to the bulk passing the amorphous/crystal interface. That is, the damaged layer was recovered with good crystallinity.

It is noted that recombination centers are present in the depletion region in Ga sample, though the amorphous layer was almost completely recovered.

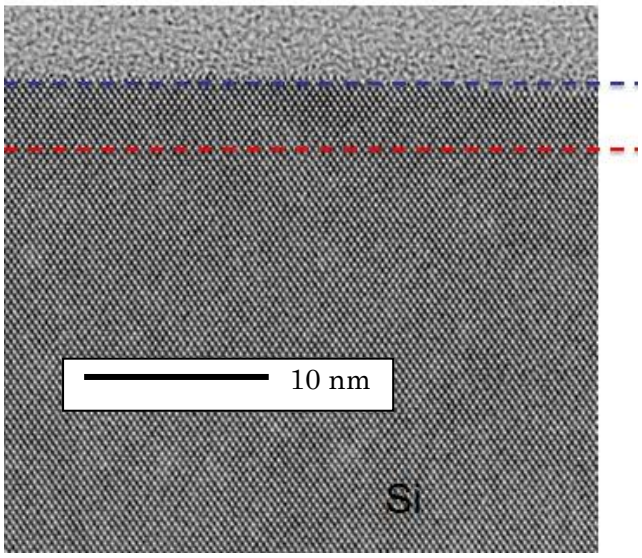

Fig. 8 TEM micrograph of BF_2 sample (dose of $3.0\text{x}10^{13}\text{cm}^{-2}$) after anneal.

Figure 10 shows the TEM micrograph of In sample. It is found that extra mono-layer is inserted with the angle of 53.8 degree, which is very near the angle of the (111) face to the (100) face. Thus, this crystal defect is located on the (111) face. This defect may be the stacking fault, originating in the In ion above solid solubility.

It is noted that the peak concentration ($\sim 1.0\text{x}10^{19}\text{cm}^{-3}$) of In at the depth of projected range exceeds the solubility of In in Si ($1.5\text{x}10^{18}\text{cm}^{-3}$ at 900C). .

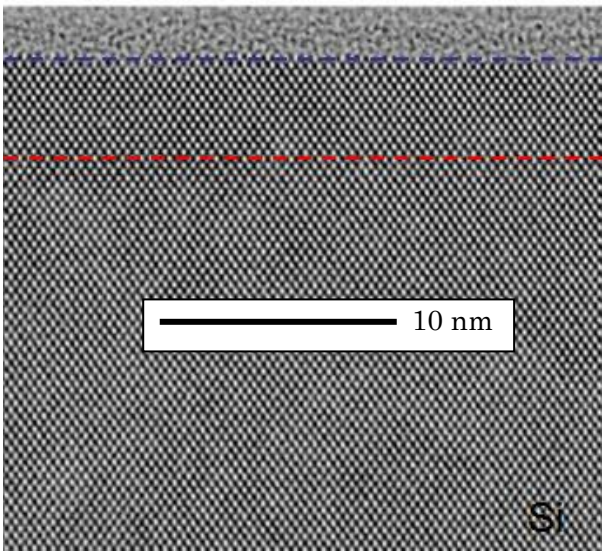

Fig. 9 TEM micrograph of Ga sample (dose of $3.0x10^{13}cm^{-2}$) after anneal.

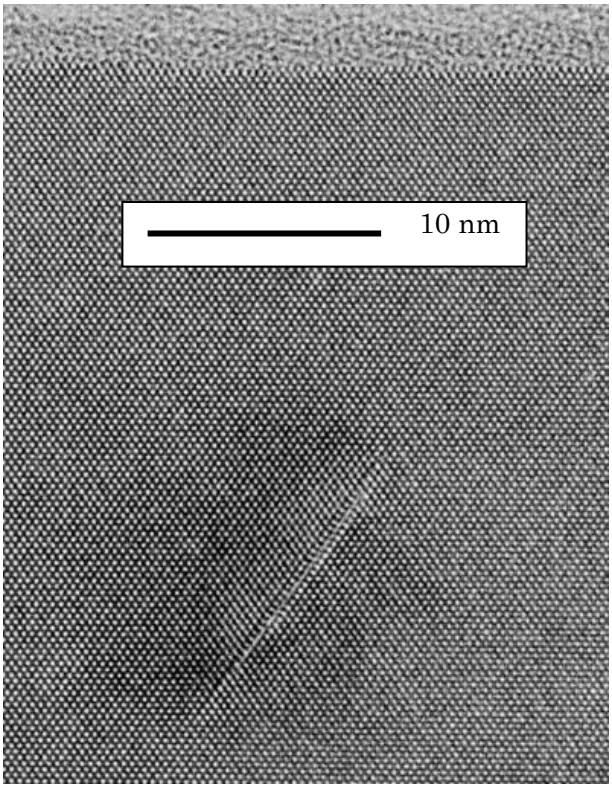

Fig. 10 TEM micrograph of In sample (dose of $3.0x10^{13}cm^{-2}$) after anneal.

4. Conclusions

Electrical characteristics by Hall-effect measurement, diode I-V characteristics and TEM analysis have been investigated for BF_2, Ga and In implanted Si under halo implant conditions. BF2 samples have good forward current characteristics, while Ga and In samples show the recombination current at the low voltage. BF2 and Ga samples have lower reverse current, while In samples have larger reverse current. This trend disagrees with the results of the JPV method.

References

[1] Sawada et al., Solid State Devices and Materials-2008, B-8-4, p.874
[2] H. Park, S. Todorov, B. Colombeau, D. Rodier, D. Kouzminov, W. Zou, B. Guo, N. Khasgiwale, and K. Decker-Lucke, IIT-2012
[3] B. Wo, Y. Matsunaga, S. Aid, S. Matsumoto, J. Borland, and M/ Tanjo, IIT-2012
[4] J. Borland, M. Tanjo, S. Sakai, T. Nagayama, H. Kiyama, and K. Suguro, IWJT-2012
[5] S. M. Sze, in Physics of Semiconductor Devices, (A Wiley-International Publication)